Ferroelectric control of magnetism in BaTiO$_3$/Fe heterostructures via interface strain coupling

Sarbeswar Sahoo, Srinivas Polisetty, Chun-Gang Duan, Sitaram S. Jaswal, Evgeny Y. Tsymbal, and Christian Binek*

Department of Physics and Astronomy and the Nebraska Center for Materials and Nanoscience,
University of Nebraska, Lincoln, Nebraska 68588-0111, USA

Reversible control of magnetism is reported for a Fe thin film in proximity of a BaTiO$_3$ single crystal. Large magnetization changes emerge in response to ferroelectric switching and structural transitions of BaTiO$_3$ controlled by applied electric fields and temperature, respectively. Interface strain coupling is the primary mechanism altering the induced magnetic anisotropy. As a result, coercivity changes up to 120% occur between the various structural states of BaTiO$_3$. Up to 20% coercivity change is achieved via electrical control at room temperature. Our all solid state ferroelectric-ferromagnetic heterostructures open viable possibilities for technological applications.

PACS number(s): 75.80.+q, 75.70.−i, 77.84.−s

The phenomenon of coupling between ferroic (magnetic, electric, and elastic) order parameters and their extrinsic control has recently become an exciting research area within the context of "multiferroics and magnetoelectrics."[1–30] These materials exhibit simultaneous presence and sometimes significant coupling of ferroic order parameters. Conjugate magnetic and electric fields can be used to manipulate the respective cross coupled order parameter. Switching of a ferromagnetic (FM) order by an electric field, for instance, promises significant impact in the design of next generation of devices. Most recently studied multiferroics and magnetoelectrics can be classified into two kinds of systems: single-phase systems and two-phase systems. Single-phase multiferroics[8–16] are predicted to be rare;[2] however, many perovskite-type oxides have successfully been exploited to control the magnetic order by electrical means and vice versa. Because of their chemical and structural complexities, the details of coupling of ferroelectric and magnetic properties of such systems are currently not well understood.

The majority of two-phase multiferroics[17–30] include artificially grown ferroelectric (FE)-FM heterostructures such as BaTiO$_3$/La$_{0.66}$Sr$_{0.33}$MnO$_3$ (BTO/LSMO), BiFeO$_3$/SrTiO$_3$, nanopillar embedded structures of BTO-CoFe$_2$O$_4$ or BiFeO$_3$-CoFe$_2$O$_4$, Pb(Zr,Ti)O$_3$/CoPd, Pb(Zr,Ti)O$_3$/terfenol-D, etc. By using BTO/LSMO, Lee *et al.* showed that lattice distortions during the structural phase transitions of BTO can cause changes in the resistivity and magnetic properties of LSMO.[17] Recently, Eerenstein *et al.* confirmed the above results and demonstrated converse magnetoelectric effects.[24] In all these studies the magnetic material is always an oxide based ferromagnet. The observed magnetic, resistive, and converse magnetoelectric effects are primarily attributed to the strain induced coupling at the interface.

Surprisingly, however, the modification of magnetic properties of a FM transition metal film, e.g., Fe film in contact with a ferroelectric such as BaTiO$_3$, has never been studied so far. Only recently, first-principle calculations predicted a magnetoelectric effect in BaTiO$_3$/Fe driven by the FM-FE interface bonding which results in changing the effective magnetic moments of Fe and Ti atoms.[30]

In this Brief Report, we study the generic and intriguing system comprised of simple itinerant FM Fe thin film on a single-crystal BTO. We systematically explore the modification in Fe film magnetism as BTO undergoes various structural phase transitions as well as the so-called converse magnetoelectric effect in this heterostructure. The observed effects are significantly enhanced compared to other multiferroics involving complex FM oxides and also electrochemically prepared heterostructures.[31]

BaTiO$_3$ is the most extensively investigated FE material which, even today, is widely used in practical applications. The structural properties of this archetypical FE are well established.[32,33] It exhibits three distinct structural phase transitions: cubic-tetragonal (C-T) at a temperature $T \approx 393$ K, tetragonal-orthorhombic (T-O) at $T \approx 278$ K, and orthorhombic-rhombohedral (O-R) at $T \approx 190$ K, respectively. Fe is a classical 3d metal which has a Curie temperature $T_C = 1043$ K and exhibits bcc structure in its most stable form.

We deposited a 10 nm thick Fe film on a single-crystal BaTiO$_3$ (100) substrate by molecular beam epitaxy at a base pressure of 5×10^{-11} mbar. During growth of the Fe film, the substrate was heated to and maintained at $T = 373$ K. This stabilizes the tetragonal structure of BTO and consequently maintains its ferroelectric polarity. θ-2θ x-ray diffraction and pole figure scans reveal the polycrystalline nature of the top Fe film.

The magnetic response of the BTO/Fe heterostructure with variation in temperature, measured by the use of a superconducting quantum interference device magnetometer (Quantum Design, MPMS-XL), is presented in Fig. 1. The temperature dependence of the in-plane magnetization, $M_\parallel$ vs T, was measured in small magnetic fields of $\mu_0 H = 2$ and 8 mT after cooling from $T = 400$ K to $T = 5$ K in a saturation field of $\mu_0 H = 0.8$ T applied in the plane of the sample, i.e., in the (100) plane of BTO.

$M_\parallel$ vs T heating and cooling branches exhibit distinct anomalies and concomitant thermal hysteresis at T-O and O-R transitions. This unequivocally indicates that the magnetic properties of the top Fe film are strongly modified by the BTO lattice distortions during its structural phase transitions via magnetoelastic coupling at the interface. The magnetoelastic energy gives rise to a uniaxial anisotropy.[34] The stress anisotropy energy reads $E_{me} = K_{me} \sin^2 \theta$, where $K_{me} = \frac{3}{2}\lambda\sigma$. λ is the average magnetostriction coefficient quanti-
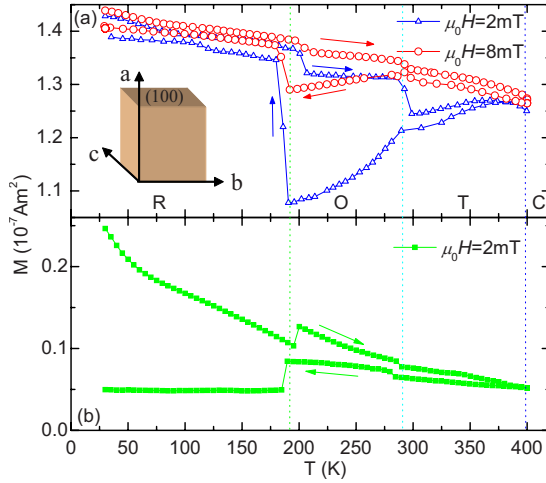
FIG. 1. (Color online) (a) Variation of the Fe film in-plane magnetization, $M_\parallel$, with temperature, T, at magnetic fields, $\mu_0 H$ =2 mT (triangles) and 8 mT (circles). The arrows point to the direction of temperature scans. Letters R, O, T, and C denote the rhombohedral, orthorhombic, tetragonal, and cubic states of BaTiO$_3$ single-crystal substrate, respectively. The dotted lines are the boundaries between respective transitions. The inset depicts a representative BTO unit cell with reference axes. (b) $M_\perp$ vs T curves at $\mu_0 H$=2 mT.

fying the relative length change of the sample between the demagnetized and magnetized states, σ is the induced stress, and θ is the angle between $\vec{M}$ and σ-axis. Obviously K_{me} >0 favors θ=0 which means parallel alignment of the magnetization relative to the stress axis while K_{me}<0 favors perpendicular alignment with $\theta=\pi/2$.

In the heating branch of $M_\parallel$ vs T at $\mu_0 H$=2 mT, there are sharp discontinuities in $M_\parallel$ where changes of $\left| \Delta M_\parallel / M_\parallel \right|$ ≈4% and ≈5% were observed at R→O and O→T transitions, respectively. Since λ is negative at the saturation field of $\mu_0 H$=0.8 T and of the order of 10^{-6} for polycrystalline Fe,[34] drops in $M_\parallel$ values at these transitions signify tensile strain (σ>0) induced by BTO in the Fe film. This is consistent with the temperature driven changes in the lattice parameters of BTO/Fe interface area. The inset to Fig. 1(a) depicts a representative BaTiO$_3$ unit cell with the reference axes (a,b,c) and the (100) plane. Heating leads to an increase in b=c during the R→O transition. This gives rise to biaxial tensile stress[17,32] which causes the drop in magnetization at the R→O transition. The correlation between structure and magnetism becomes more involved at the O→T transition due to a complex distribution of tensile and compressive stresses originating from structural twin domains in the O phase[32,33] as discussed below.

For $\lambda\sigma$<0, the in-plane stress induced by BTO on the Fe film somewhat favors the magnetization to be perpendicular to the film plane. This is evidenced by measurements of the perpendicular component $M_\perp$ vs T where the applied magnetic field is oriented perpendicular to the sample plane. Figure 1(b) shows the corresponding increase of $M_\perp$ vs T at the R→O transition. The gain in the out-of-plane magnetization originates from the magnetization loss in the in-plane com-

ponent. As noticed from Fig. 1(a) the associated features at $\mu_0 H$=8 mT are less pronounced than those at $\mu_0 H$=2 mT. This is in accordance with the fact that stronger Zeeman fields saturate the Fe magnetization and stabilize the latter along the field direction leading to reduced effects at BTO phase transitions. Indeed, at a field of $\mu_0 H$=50 mT all transitions completely disappear, while at $\mu_0 H$=5 mT the magnetic moment values lie intermediate between those of the $\mu_0 H$=2 mT and $\mu_0 H$=8 mT (both 50 and 5 mT data not shown).

In contrast to the heating branch, the $M_\parallel$ vs T cooling branch exhibits a gradual T→O transition and a predominant O→R transition accompanied with $\left| \Delta M_\parallel / M_\parallel \right| \approx 25\%$ at $\mu_0 H$=2 mT. Interestingly, the most apparent changes in $M_\parallel$ vs T curves occur in the O phase and at O→R transition, i.e., in the O phase $M_\parallel$ decreases with decreasing T while it sharply increases at the O→R transition. The former indicates that on cooling the stress axis becomes magnetically harder which is due to the tensile stress induced by BTO, i.e., $d\sigma/dT$<0. This is corroborated by the out-of-plane $M_\perp$ vs T curve which shows a corresponding increase in magnetization. The rise of $M_\parallel$ at the O→R transition implies a very pronounced change from magnetically harder to easier axis behavior during cooling. The magnetization of the various $M_\parallel$ vs T curves retains its value at low temperatures in the structurally highly symmetric R phase. Here the in-plane lattice parameters are reduced with respect to the O phase giving rise to compressive strain (σ<0), hence, generating an easy in-plane magnetization behavior.

The differences in behaviors between heating and cooling curves discussed above may be related to the twining of BTO in the O phase. Similar features have been observed in the electric resistivity vs temperature.[17] It is well known that BTO exhibits two possible twinning states with equal probability in the O state,[32,33] however, they differ by 90° monoclinic planes which may lead to compression or tension at the interface. The development of either type of twining depends on the condition of minimum strain and distortions of crystal boundaries[32,33] which in turn is determined by the thermal history of the O-T transition either upon cooling or heating.

In-plane magnetic hysteresis loops measured at various temperatures reveal profound changes in the coercivity, $\mu_0 H_c$, and the ratio of remanent to saturation magnetization, M_r/M_s, of the Fe film as plotted in Figs. 2(a) and 2(b). This implies, again, the dramatic sensitivity of the Fe magnetic properties on the in-plane lattice distortions in the underlying BTO. Note that the loops were measured while sequentially decreasing the temperature. We find the changes in coercivity of $\left| \Delta H_c / H_c \right| \approx 20\%$ and ≈120% at T→O and O→R transitions, respectively. Quite predictably, the remanent magnetization follows the tendency of the cooling branch in Fig. 1(a) with $\left| \Delta M_r / M_s \right| \approx 33\%$ at the O→R transition. These results, firstly, corroborate the $M_\parallel$ vs T behavior in Fig. 1(a); secondly, signify the importance of the direction of temperature scan approaching the respective transitions in determining the twinning of BTO.

The voltage control of coercivity of a multiferroic material is extremely attractive for applications because of the lower power consumption compared to its current-controlled
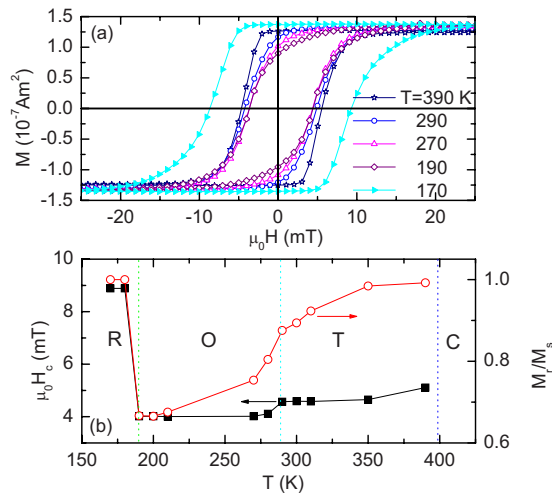
FIG. 2. (Color online) (a) Magnetic hysteresis loops measured at various temperatures $170\ \mathrm{K} \leqslant T \leqslant 390\ \mathrm{K}$. (b) $\mu_0 H_c$ (squares) and M_r/M_s (circles) vs T as obtained from the loops in (a).

FIG. 3. (Color online) (a) Normalized Kerr magnetic loops at room temperature measured at different applied electric fields $-10\ \mathrm{kV/cm} < E < 10\ \mathrm{kV/cm}$. (b) $\mu_0 H_c$ vs E as obtained from loops in (a). The arrows point to directions along which the change of electric fields takes place in steps.

counterparts. Furthermore such a heterostructure can provide an alternative to heat assisted magnetic recording for the future high-density recording media. Figure 3(a) shows the longitudinal magneto-optic Kerr effect loops revealing the control of $\mu_0 H_c$ by the application of an electric field, E. The electric field was applied across ~ 0.5 mm thick BTO/Fe by using gold wires with silver paste contacts at the bottom of BTO and covering up to half of the top Fe film (4×5 mm^2). The laser beam was focused on the clear half of Fe film. The electric field was changed from $E = -10$ kV/cm up to $E = 10$ kV/cm in ascending steps and then descending back to $E = -10$ kV/cm along the arrows shown in Fig. 3(b). $\mu_0 H_c$ is maximum in the remanent state of BTO and drops symmetrically [in accordance with $\sigma(E) = \sigma(-E)$] by $|\Delta H_c/H_c| \approx 20\%$ for $|E|$ above the FE coercivity of BTO. The hysteretic behavior around low E regions is believed to be associated with the incomplete rotation of BTO domains. This coercivity change is significantly larger
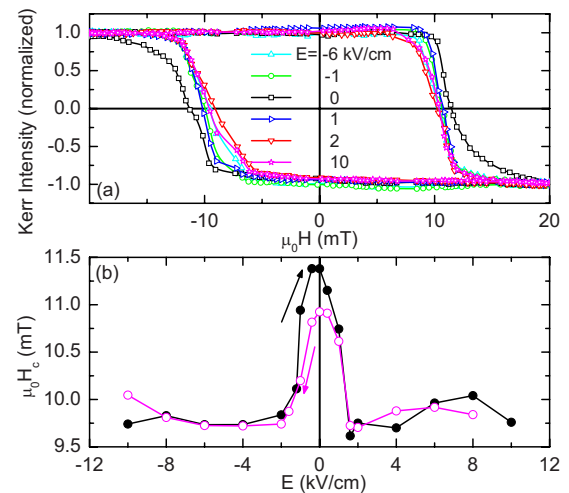
than those recently reported in FePt and FePd thin films immersed in an electrolyte.[31] Therefore, our all solid state structure is more attractive for device applications.

In conclusion, we find that the magnetic properties of a simple $3d$ transition metal ferromagnetic thin film can be strongly altered in proximity with a single-crystal ferroelectric. We demonstrate electric and thermal control of magnetic anisotropy and coercivity by studying a classical ferroelectric-ferromagnetic BaTiO$_3$/Fe heterostructure. Simplicity of our all solid state heterostructure and strength of the observed effects promise significant potential for future spintronic applications.

*cbinek2@unl.edu

[1] W. Eerenstein, N. D. Mathur, and J. F. Scott, Nature (London) **442**, 759 (2006).

[2] N. A. Hill, J. Phys. Chem. B **104**, 6694 (2000).

[3] C. Ederer and N. A. Spaldin, Nat. Mater. **3**, 849 (2004).

[4] N. A. Spaldin and M. Fiebig, Science **309**, 391 (2005).

[5] Ch. Binek and B. Doudin, J. Phys.: Condens. Matter **17**, L39 (2005).

[6] E. Y. Tsymbal and H. Kohlstedt, Science **313**, 181 (2006).

[7] M. Fiebig, J. Phys. D **38**, R123 (2005).

[8] T. Kimura, T. Goto, H. Shintani, K. Ishizaka, T. Arima, and Y. Tokura, Nature (London) **426**, 55 (2003).

[9] N. Hur, S. Park, P. A. Sharma, J. S. Ahn, S. Guha, and S.-W. Cheong, Nature (London) **429**, 392 (2004).

[10] M. Gajek, M. Bibes, S. Fusil, K. Bouzehouane, J. Fontcubert, A. Barthélémy, and A. Fert, Nat. Mater. **6**, 296 (2007).

[11] T. Kimura, S. Kawamoto, I. Yamada, M. Azuma, M. Takano, and Y. Tokura, Phys. Rev. B **67**, 180401(R) (2003).

[12] T. Lottermoser, T. Lonkai, U. Amann, D. Hohlwein, J. Ihringer, and M. Fiebig, Nature (London) **430**, 541 (2004).

[13] J. Hemberger, P. Lunkenheimer, R. Fichtl, H.-A. Krug von Nidda, V. Tsurkan, and A. Loidl, Nature (London) **434**, 364 (2005).

[14] Y. Yamasaki, S. Miyasaka, Y. Kaneko, J. P. He, T. Arima, and Y. Tokura, Phys. Rev. Lett. **96**, 207204 (2006).

[15] C. Thiele, K. Dörr, O. Bilani, J. Rödel, and L. Schultz, Phys. Rev. B **75**, 054408 (2007).

[16] T. Zhao, A. Scholl, F. Zavaliche, K. Lee, M. Barry, A. Doran, M. P. Cruz, Y. H. Chu, C. Ederer, N. A. Spaldin, R. R. Das, D. M. Kim, S. H. Baek, C. B. Eom, and R. Ramesh, Nat. Mater. **5**, 823 (2006).

[17] M. K. Lee, T. K. Nath, C. B. Eom, M. C. Smoak, and F. Tsui, Appl. Phys. Lett. **77**, 3547 (2000).

[18] J. Wang, J. Neaton, H. Zheng, V. Nagarajan, S. B. Ogale, B. Liu, D. Viehland, V. Vaithyanathan, D. G. Schlom, U. Waghmare, N. A. Spaldin, K. M. Rabe, M. Wuttig, and R. Ramesh, Science **299**, 1719 (2003).

[19] H. Zheng, J. Wang, S. E. Lofland, Z. Ma, L. Mohaddes-Ardabili, T. Zhao, L. Salamanca-Riba, S. R. Sinde, S. B. Ogale, F. Bai, D. Viehland, Y. Jia, D. G. Schlom, M. Wuttig, A. Roytburd, and R. Ramesh, Science **303**, 661 (2004).

[20] F. Zavaliche, H. Zheng, L. Mohaddes-Ardabili, S. Y. Yang, Q. Zhan, P. Shafer, E. Reilly, R. Chopdekar, Y. Jia, P. Wright, D. G. Schlom, Y. Suzuki, and R. Ramesh, Nano Lett. **5**, 1793 (2005).

[21] P. Borisov, A. Hochstrat, X. Chen, W. Kleemann, and Ch. Binek, Phys. Rev. Lett. **94**, 117203 (2005).

[22] V. Laukhin, V. Skumryev, X. Marti, D. Hrabovsky, F. Sanchez, M. V. Garcia-Cuenca, C. Ferrater, M. Varela, U. Luders, J. F. Bobo, and J. Fontcuberta, Phys. Rev. Lett. **97**, 227201 (2006).

[23] H. Bea, M. Bibes, M. Sirena, G. Herranz, K. Bouzehouane, E. Jacquet, S. Fusil, P. Paruch, and M. Dawber, Appl. Phys. Lett. **88**, 062502 (2006).

[24] W. Eerenstein, M. Wiora, J. L. Prieto, J. F. Scott, and N. D. Mathur, Nat. Mater. **6**, 348 (2007).

[25] S. Geprägs, M. Opel, S. T. B. Goennenwein, and R. Gross, Philos. Mag. Lett. **87**, 141 (2007).

[26] X. Qi, H. Kim, and M. G. Blamire, Philos. Mag. Lett. **87**, 175 (2007).

[27] S.-K. Kim, J.-W. Lee, S.-C. Shin, H. W. Song, C. H. Lee, and K. No, J. Magn. Magn. Mater. **267**, 127 (2003).

[28] G. Srinivasan, E. T. Rasmussen, J. Gallegos, R. Srinivasan, Yu. I. Bokhan, and V. M. Laletin, Phys. Rev. B **64**, 214408 (2001).

[29] D. Dale, A. Fleet, J. D. Brook, and Y. Suzuki, Appl. Phys. Lett. **82**, 3725 (2003).

[30] C.-G. Duan, S. S. Jaswal, and E. Y. Tsymbal, Phys. Rev. Lett. **97**, 047201 (2006).

[31] M. Weisheit, S. Fähler, A. Marty, Y. Souche, C. Poinsignon, and D. Givord, Science **315**, 349 (2007).

[32] H. F. Kay and F. Vousden, Philos. Mag. **40**, 1019 (1949).

[33] R. G. Rhodes, Acta Crystallogr. **4**, 105 (1951).

[34] B. D. Cullity, *Introduction to Magnetic Materials* (Addision-Wesley, Reading, MA, 1972).